Sensors and Actuators A 241 (2016) 190–196

Contents lists available at ScienceDirect

Sensors and Actuators A: Physical

journal homepage: www.elsevier.com/locate/sna

Solution refractive index sensor based on high resolution total-internal-reflection heterodyne interferometry

Jiun-You Lin

Department of Mechatronics Engineering, National Changhua University of Education, No. 2, Shi-Da Road, Changhua City 50074, Taiwan, ROC

ARTICLE INFO

Article history:
Received 22 December 2015
Accepted 7 February 2016
Available online 9 February 2016

Keywords:
Solution refractive index
High resolution
Total internal reflection
Heterodyne interferometry

ABSTRACT

In this paper, a solution refractive index sensor is proposed based on a high resolution total-internal-reflection (TIR) interferometry. In the proposed sensor, a half-wave plate and a quarter-wave plate that exhibit specific optic-axis azimuths are combined to form a phase shifter. When an isosceles right-angle prism whose base contacts with a tested solution is placed between the phase shifter and an analyzer with suitable transmission-axis azimuth, it shifts and increases the phase difference of the s- and p-polarization states at one TIR. The increased phase difference relates to the solution refractive index; thus it can be easily and accurately measured by evaluating the phase difference. The feasibility was demonstrated by experimental results. This method has the merits of both common-path interferometry and heterodyne interferometry.

1. Introduction

Accurate measurements of solution refractive index (RI) are often needed in biochemical analysis and clinic monitoring. Many optical reflection techniques have been developed for measuring solution refractive index, such as Brewster angle methods [1,2], total internal reflection (TIR) interferometry [3–5], differential refractometry [6], and surface plasmon resonance (SPR) technique [7–9]. The Brewster angle method estimates the refractive index of a solution by measuring the reflectance of polarized light from a sample surface near the Brewster angle, and the system yielded a measurement resolution of nearly 10^{-4} RIU. In the TIR interferometry, the refractive index is inferred from the TIR phase difference between two interference signals. The method showed a detection limit of approximately $10^{-3} - 10^{-5}$ RIU. The differential refractometry uses a linear diode array to detect the angular distribution of the intensity of a divergent light beam reflected from the prism-sample interface. The desired refractive index is estimated by measuring the critical angle obtained from the curve of the ratio of the incident and reflected light intensities. A high resolution of better than 3×10^{-6} RIU from this method was achieved. The SPR technique determines the refractive index by measuring the SPR reflectance, phase or wavelength shifts of an associated light beam. The technique can achieve an excellent measurement resolution superior to 10^{-5} RIU.

In this paper, an optical sensor is proposed for measuring solution refractive index using high resolution TIR heterodyne interferometric technique. A linearly heterodyne light propagates through a phase shifter, consisting of a half-wave and a quarter-wave plate, subsequently penetrating an isosceles right-angle prism with a solution at an angle larger than the critical angle. The light in the prism undergoes one TIR, finally traveling through an analyzer to extract the interference signal of the *p*- and *s*-polarized light. When the azimuth angles of the phase shifter wave plates are properly selected, the final phase difference exhibited by the solution refractive index of the interference signal is linked to the azimuth angle of the analyzer transmission axis. The final phase difference can be greatly enhanced by regulating the azimuth angle of the analyzer. The enhanced phase difference is easily measurable using heterodyne interferometric technique. Hence the refractive index is accurately obtainable from the data of the measured phase difference. Compared to the previous study [10], the TIR apparatus proposed here uses less number of wave plates, thereby simplifying the optical configuration and reducing the fabrication cost. The feasibility of this method was demonstrated by the experimental results, which yielded measurement sensitivity and resolution levels of approximately 10^4 (deg/RIU) and1.2 to 2.5 $\times 10^{-5}$ RIU at the measurement range of 1.332 – 1.341.

E-mail address: jylin@cc.ncue.edu.tw

http://dx.doi.org/10.1016/j.sna.2016.02.020
0924-4247/

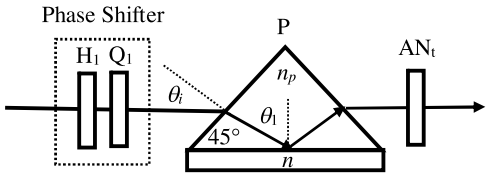

Fig. 1. The solution refractive index measurement apparatus.

2. Principle

2.1. Phase difference resulting from high resolution TIR apparatus

Fig. 1 demonstrates the optical configuration of the high resolution TIR apparatus. For convenience, the +*z* axis is set in the direction of the propagation of light and the *x* axis is perpendicular to the plane of the paper. A linearly polarized light whose light polarization plane is properly set at an angle θ_p from the *x* axis exhibits the following Jones vector:

$$E_i = \begin{pmatrix} \cos\theta_p \\ \sin\theta_p \end{pmatrix}. \tag{1}$$

The light is guided to pass through a phase shifter, comprising a half-wave plate H_1 (with fast axis at a $\Delta/2$ angle to the *x*-axis) and a quarter-wave plate Q_1 (with fast axes at 45° respect to *x*-axis), and is subsequently incident at θ_i on one side of an isosceles right-angle prism P with refractive index n_p. The prism is mounted on a rotation stage. The hypotenuse of the prism is contacted with a tested solution of refractive index *n*. The light beam penetrates into the prism at an incidence angle of θ_1 onto the prism/solution interface. The relation between the angles θ_i and θ_1 can be determined as follows:

$$\theta_1 = 45^\circ + \sin^{-1}\left(\frac{\sin\theta_i}{n_p}\right). \tag{2}$$

When θ_i exceeds θ_{ic}, which is the angle that makes θ_1 equal the critical angle θ_{1c}, the light is completely reflected at the prism/tested solution interface. The light output from the prism travels through an analyzer AN_t (the transmission axis is β to the x-axis) for interference. The amplitude E_i becomes E_t, as follows:

$$E_t = \begin{pmatrix} \cos^2\beta & \sin\beta\cos\beta \\ \sin\beta\cos\beta & \sin^2\beta \end{pmatrix} \begin{pmatrix} t_p t'_p \exp(-i\delta/2) & 0 \\ 0 & t_s t'_s \exp(-i\delta/2) \end{pmatrix} \frac{1}{\sqrt{2}} \begin{pmatrix} 1 & -i \\ -i & 1 \end{pmatrix} \times \begin{pmatrix} \cos\Delta & \sin\Delta \\ \sin\Delta & -\cos\Delta \end{pmatrix} \begin{pmatrix} \cos\theta_p \\ \sin\theta_p \end{pmatrix} = (A_{t1}\cos\theta_p \exp(i\phi) + A_{t2}\sin\theta_p \exp(i\pi/2)) \begin{pmatrix} \cos\beta \\ \sin\beta \end{pmatrix} \tag{3}$$

where the amplitudes A_{t1} and A_{t2} can be written as follows:

$$A_{t1} = \left\{ \frac{1}{2}[(t_p t'_p \cos\beta)^2 + (t_s t'_s \sin\beta)^2 + t_p t'_p t_s t'_s \sin 2\beta \cdot \sin(2\Delta + \delta)] \right\}^{1/2}, \tag{4}$$

$$A_{t2} = \left\{ \frac{1}{2}[(t_p t'_p \cos\beta)^2 + (t_s t'_s \sin\beta)^2 - t_p t'_p t_s t'_s \sin 2\beta \cdot \sin(2\Delta + \delta)] \right\}^{1/2}, \tag{5}$$

and the phase difference φ can be expressed as follows:

$$\begin{aligned} \phi = {} & \tan^{-1}[-\tan(45^\circ - \sigma)\cdot\tan(\Delta + \delta/2 - \pi/4)] \\ & - \tan^{-1}[-\tan(45^\circ + \sigma)\cdot\tan(\Delta + \delta/2 - \pi/4)] \end{aligned}. \tag{6}$$

In Eqs. (3)–(6), δ is the phase difference between the *s*- and *p*-polarizations of one TIR at the prism-solution interface; (t_p, t_s) and (t'_p, t'_s) are the transmission coefficients at the air-prism and prism-air interfaces, respectively; Δ and σ are the parameters introduced using the phase shifter and analyzer AN_t, respectively. δ and σ can be derived using Fresnel's equations and Jones matrix calculation [11]:

$$\delta = 2\tan^{-1}\left\{ \frac{\left[\sin^2\left[45^\circ + \sin^{-1}\left(\sin\theta_i/n_p\right)\right] - (n/n_p)^2\right]^{1/2}}{\tan\left[45^\circ + \sin^{-1}(\sin\theta_i/n_p)\right]\cdot\sin\left[45^\circ + \sin^{-1}(\sin\theta_i/n_p)\right]} \right\}, \tag{7}$$

$$\sigma = \tan^{-1}\left(\frac{t_s t'_s}{t_{p'} t'_p}\tan\beta\right), \tag{8}$$

and the transmission coefficients are determined as follows:

$$t_p = \frac{2\cos\theta_i}{n_p\cos\theta_i + \left[1 - (\sin\theta_i/n_p)^2\right]^{1/2}}, \tag{9}$$

$$t_s = \frac{2\cos\theta_i}{\cos\theta_i + n_p\left[1 - (\sin\theta_i/n_p)^2\right]^{1/2}}, \tag{10}$$

$$t'_p = \frac{2n_p\left[1 - \left(\sin\theta_i/n_p\right)^2\right]^{1/2}}{n_p\cos\theta_i + \left[1 - \left(\sin\theta_i/n_p\right)^2\right]^{1/2}}. \tag{11}$$

$$t'_s = \frac{2n_p\left[1 - (\sin\theta_i/n_p)^2\right]^{1/2}}{\cos\theta_i + n_p\left[1 - (\sin\theta_i/n_p)^2\right]^{1/2}}, \tag{12}$$

Eqs. (6)–(12) indicates that the phase difference φ depends on the parameters of Δ,σ, *n*, n_p, and θ_i. If the values of σ, Δ, *n*, and n_p are specific, the phase difference φ is a function of the incident angle θ_i. When the parameter σ (determined by the value of β) is set toward 45°, the value of $\tan(45^\circ \pm\sigma)$ will become large, as shown in Eq. (6). Under the condition, proper selection of the parameter Δ can substantially increased the phase difference φ. In the proposed method, Δ is used to vary the phase level of $\delta/2$ and is determined based on the azimuth angle of the fast axis of H_1. In this method, it is set at approximately $(\pi/4 - \delta_{,\max}/4)$, where $\delta_{\max}$ denotes the maximal value of the phase difference δ and is expressed as follows [12]:

$$\delta_{\max} = 2\tan^{-1}\left(\frac{(n_p/n)^2 - 1}{2(n_p/n)}\right). \tag{13}$$

The phase-level change allows the φ versus θ_i curve to increase the linearity, extending the variation range of the phase difference φ. This increased linearity can enhance the uniformity of the sensitivity of the φ versus θ_i curve. Fig. 2 displays the relation between the phase difference φ and incident angle θ_i at an azimuth angle of β when the conditions of $n_p = 1.77862$ and $n = 1.332$, and the calculated value $\Delta \cong \pi/4 - \delta_{\max}/4 = 36.8^\circ$ are substituted into Eqs. (6)–(12). For comparison, the relation of the phase difference δ versus the incident angle θ_i is marked as "o" in Fig. 2. The simulated results indicates that at the angles $44^\circ \le \beta \le 46^\circ$ the phase difference φ exhibits sharp and large phase-difference variations around the incident angle θ_{io} at which the phase difference $\varphi = 0^\circ$. By contrast, the curve δ indicates the condition of a small, unchangeable phase-difference variation. Additionally, Fig. 3 shows the plots of the reflection coefficients A_{t1} and A_{t2}, as exhibited in Eqs. (4) and (5). Because at the parameter $\Delta \cong \pi/4 - \delta_{\max}/4$ and the angles $44^\circ \le \beta \le 46^\circ$, the value of $[(t_p t'_p \cos\beta)^{2\pm} (t_s t'_s \sin\beta)^2]$ is close to that of $t_p t'_p t_s t'_s \sin(2\beta)\cdot\sin(2\Delta \pm \delta)$ in the vicinity of θ_{io}, the simulation therefore demonstrates that the values of A_{t1} are large and A_{t2} are small, especially at β=45°. Based on the characteristics of the distinct sharp phase-difference variation, and the dependence